COMPOSITION OF THE MARTIAN POLAR CAPS AND PLANETARY HEAT FLOW. A. Broquet[1], M. A. Wieczorek[1], and W. Fa[2], [1]Observatoire de la Côte d'Azur, Laboratoire Lagrange, Université Côte d'Azur, Nice, France (adrien.broquet@oca.eu) [2]Institute of Remote Sensing and Geographical Information System, School of Earth and Space Sciences, Peking University, Beijing, China.

Introduction: The north and south polar caps of Mars are tremendous reservoirs of ices and dust of unknown composition [1]. Both polar caps are geologically young ($<$ 10 Ma [2]) and their stratigraphically layered deposits are a witness to the planet's recent climate evolution. They act as large scale loads that can bend the basement. Analysis of the associated lithospheric flexure is one of the few methods that give access to the composition of the polar caps and to the present-day strength of the lithosphere, which is related to the thermal state of the planet [3].

In this study, we use a novel technique that combines radar and elevation data with a flexure model to probe the basement of the Martian south and north polar caps and jointly invert for their composition and the strength of the underlying lithosphere.

Methods and Data: For each polar cap, we invert for the elastic thickness of the lithosphere (T_e), the polar cap load density (ρ), and the real part of the dielectric constant (ε), by minimizing the root-mean-square of the misfit between the thickness of the polar cap predicted by a flexure model and the thickness observed by sounding radar [see also 4]. The misfit function is

$$\psi(\varepsilon, T_e, \rho) = [h_e - h_0 - W(T_e, \rho)] - h_t(\varepsilon), \quad (1)$$

where h_e is the surface elevation, h_0 is an estimated pre-loading surface topography, W is the computed deflection of the polar cap basement, and h_t is the thickness of the polar cap derived from radar data. All terms depend implicitly on position. h_0 is estimated using an annulus of surface elevation data exterior to the polar cap and these data are interpolated poleward using a minimum curvature method [5].

For the south polar cap, we picked manually 995 locations (Figure 1, right), investigated all nearby available radargrams from MARSIS (Mars Advanced Radar for Subsurface and Ionosphere Sounding) data, and identified visually the reflections arising from the icy surface and the ice/substratum interface. Following [6], gravity and topography data are also used to give bounds on the allowed T_e and ρ. This procedure involves matching the observed localized spectral ratio of the gravity and topography (i.e., the admittance) to a theoretical loading model that predicts the gravity signal based on the topography.

For the north polar cap, we picked manually 213 locations (Figure 1, left) and estimated the thickness using

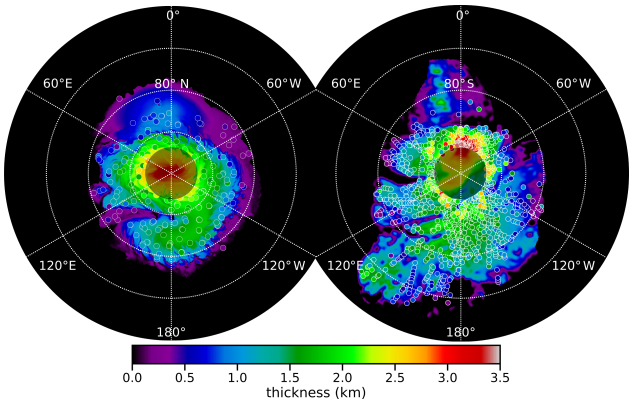

Figure 1: Estimated thickness of the north (left) and south (right) polar caps from surface elevations under the assumption that the base of the cap follows the regional slope. The filled colored circles correspond to the radar thickness (ε = 3) obtained at 213 (left) and 995 (right) regions.

MARSIS data. At the north pole, the gravity field is not used as there are important signals originating from subsurface loads that have no surface expressions [7].

Results: The inversion results for both the south and north polar caps are shown in Figure 2. The black lines and fill give a contour of the maximum allowed misfit of eq. 1, where the range of ε and ρ were limited such that they can be simultaneously obtained by mixtures of ices and dust. The green line limits the parameter space of the south pole to possible mixtures that fit the ranges of T_e and ρ given by an admittance analysis similar to [6].

In this plot, the maximum allowed misfits were set to 455 m and 266 m for the south and north polar caps, respectively. These include uncertainties from the range resolution of MARSIS (86.5 and 86.5 m), surface roughness at the scale of the Fresnel zone of MARSIS (200 and 185 m), and the uncertainty in the estimation of the pre-loading surface (400 and 170 m). The uncertainty on the pre-loading surface was estimated by varying the bounds of the polar mask that was used before interpolation.

To determine plausible mixtures of ices and dust, ε of solid CO_2, H_2O ice, and dust were set to 2.2, 3 and 6 respectively, and the densities of solid CO_2 and H_2O ice were assumed to be 1560 and 920 kg m^{-3}. The density of the dust component was allowed to vary from 2200 to 3400 kg m^{-3}, which covers the range from gypsum

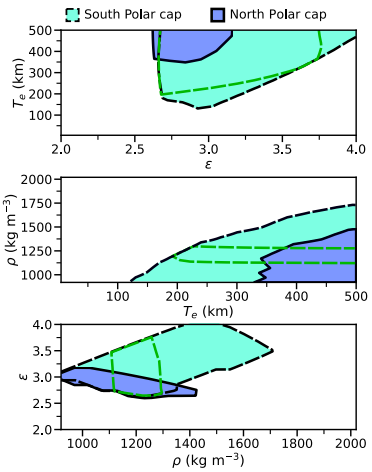

Figure 2: Inversion results for the south and north polar caps. For both polar caps, the black lines delimit possible mixtures that do not produce basal melting for a heat flow of 25 mW m^{-2}. The green line limits the parameter space of the south pole to possible mixtures that fit the ranges of T_e and ρ given by an admittance analysis [6].

to basalt. We further note that the thermal conductivity of the polar cap is strongly dependent on the relative abundances of ices and dust [6]. If the effective thermal conductivity is low enough, this could result in temperatures that would be sufficient to melt H_2O or CO_2 ices at the base of the cap. Because basal melting has not yet been observed by radar sounders, the black lines only show compositions that do not produce basal melting for a typical heat flow of 25 mW m^{-2} [3].

For the south polar cap and without gravity constraints, we observe that ε is allowed to vary from 2.6 to 4.0, T_e must be greater than 120 km, and ρ ranges from 920 to 1750 kg m^{-3}. With gravity constraints, ε ranges from 2.6 to 3.7, T_e is at least 200 km, and ρ is allowed to vary from 1100 to 1270 kg m^{-3}. For the north polar cap, we observe that ε can range from 2.6 to 3.1, T_e must be at least 330 km, and ρ is at most 1440 kg m^{-3}.

In Figure 3, we show two example ternary diagrams for the composition (in vol.%) of the south (dashed) and north (solid) polar caps that fit our constraints on ρ and ε, under the assumption that both are made of dust, H_2O and CO_2 ices. For the south polar cap, we observe a trade-off between the allowed quantity of dust, which varies from 8 to 22% and solid CO_2 that can range from 0 to 54%. The north polar cap, however, must contain at least 10% (and up to 54%) CO_2. 10% of solid CO_2 mixed within the north polar cap presents a volume of 15000 km^3 that is about 10 times larger than the massive CO_2 packs found at the south pole by [1].

Discussion and Conclusion: Using the formalism of [8] and accounting for heat-producing elements (HPE)

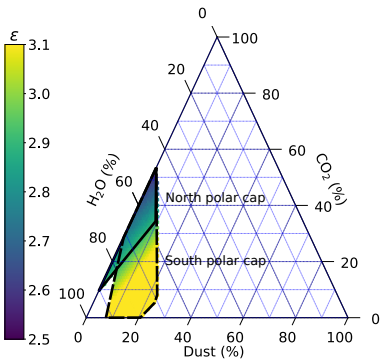

Figure 3: Ternary diagrams for the composition (in vol.%) of the north (solid) and south (dashed) polar caps based on the constraints on ρ and ε.

in the crust and mantle [3], the minimum T_e at the south and north pole can be shown to imply heat flows of 26 and 16 mW m^{-2}, respectively, which are consistent with [3]. The north polar value is significantly different from that found in [9], which is largely the result of their having mistook previously reported relative deflections between two points with the maximum absolute deflection in the center of the deposit.

In a suite of thermal evolution models, [3] investigated how the thickness of the crust (which is enriched in HPE) affects T_e. For T_e of more than 200 and 330 km at the south and north poles, only models that have an average crustal thickness of at least 62 km are compatible. If the concentration of HPE in the crust is doubled with respect to its nominal value, one model with a lower crustal thickness (29.5 km) also satisfies our constraints.

We observe a trade-off in the composition of the south polar cap between the dust and dry ice component. An independent estimate on the quantity of dust within the south polar cap could help place better constraints on the amount of sequestered dry ice. The inferred composition of the north polar cap implies that there must be at least 10% solid CO_2 mixed within the cap. Adding some dust would require an even larger solid CO_2 content. Because of the strong feedback between the polar caps and the atmosphere, having a substantial amount of sequestered CO_2 has important implications on the reconstruction of the climate evolution of the planet.

References: [1] Phillips R. J. et al. (2011) *Science, 332*, 838–841. [2] Herkenhoff K. E. and Plaut J. J. (2000) *Icarus, 144*, 243–253. [3] Plesa A.-C. et al. (2018) *GRL, 45*, 12,198–12,209. [4] Broquet A. et al. (2020) *Submitted to GRL*. [5] Smith W. H. F. and Wessel P. (1990) *Geophysics, 55*, 293–305. [6] Wieczorek M. A. (2008) *Icarus, 196*, 506–517. [7] Ding M. et al. (2019) *JGR,124*, 3095–3118. [8] McNutt M. K. (1984) *JGR, 89*, 180–194. [9] Ojha L. et al. (2019) *GRL,46*, 12756–12763.